A Gridding Algorithm for Efficient Density Compensation of Arbitrarily Sampled Fourier-Domain Data

Wasim Q. Malik, Hammad A. Khan, David J. Edwards, and Christopher J. Stevens
Department of Engineering Science, University of Oxford, Parks Road, Oxford OX1 3PJ, U.K.
Email: {wasim.malik, hammad.khan, david.edwards, christopher.stevens}@eng.ox.ac.uk

***Abstract*— Uniformly sampled data is sometimes not directly available in engineering applications ranging from synthetic aperture radars to magnetic resonance imaging. However, certain signal processing techniques such as the fast Fourier transform cannot be applied to non-equispaced data. It is therefore desirable to resample the data on a regular grid. Various interpolation schemes have been proposed for this purpose, such as gridding reconstruction. A computationally expensive step in the gridding algorithm is the estimation of the data sampling density. This paper presents a method for improving both the efficiency and the quality of gridding density estimation based on partial Voronoi diagrams. It is shown that significantly higher computational efficiency is achieved by this method over the existing schemes. Lower spreading and greater sidelobe suppression of the point spread function demonstrate the superiority of the proposed reconstruction method.**

***Index Terms*—Density estimation, gridding, non-uniform sampling, synthetic aperture imaging, Voronoi.**

I. Introduction

Hardware constraints and other design considerations of an acquisition process may result in non-uniformly sampled Fourier-domain data. This situation can arise in a variety of applications, such as radio astronomy, medical imaging, computer graphics, video transmission, and the numerical solution of partial differential equations. In the context of radars and communications, this phenomenon may occur in multi-antenna or synthetic aperture imaging systems [1, 2]. Radars, sonars and sensors with a large coverage area often sound the environment through single-element emitters mounted on airplanes or ships, forming non-uniform, sparse arrays defined by the trajectory of motion [3]. Stationary antenna elements in multiple-input multiple-output (MIMO) radar and radio imaging systems may be non-uniformly distributed due to constraints on element locations [4]. Also, an otherwise uniform acquisition process suffering from a low signal-to-noise ratio (SNR) may lose some of the Fourier-space samples effectively creating an arbitrary sampling pattern.

This poses a problem in the application of efficient signal processing techniques that require equispaced data such as the fast Fourier transform (FFT) [5] or back-propagation imaging algorithms. Several reconstruction methods have been developed to process non-uniform samples ranging from coordinate transformation [6] to interpolation [7, 8]. Another popular technique is gridding, in which non-uniform data is transformed to a regular, Cartesian grid before applying the FFT [9, 10]. The original form of gridding, used first in radio astronomy, involved the calculation of the grid points through a summation of the neighboring points defined over a frequency-domain grid [11]. Improvements to this method involve the averaging of neighboring data [12] and Gaussian weighting [13]. Algorithms based on iterative next-neighbor regridding using rescaled matrices have been proposed recently for magnetic resonance imaging (MRI) [14].

The reconstruction grid density, the choice of a convolution kernel, and the estimation of sample density are the prime design parameters of a gridding algorithm. The convolution kernel performs appropriate weighting and data smoothing, and optimal kernel selection impacts the gridding performance [9, 15]. A denser grid reduces aliasing artifacts arising from Fourier resampling [15]. Density estimation is required to compensate for nonuniform sampling [16]. In MRI and some other applications, the Fourier-domain (or *k*-space) image acquisition trajectories are known, therefore approximate analytical density compensation functions can be determined [17-19]. It is however not possible in general to derive analytical expressions for an arbitrary sampling pattern. In such cases, the density function must be extracted from the Fourier sampling pattern itself. Recent work has addressed this problem for magnetic resonance tomography (MRT) spiral sampling patterns [20-23]. Many arbitrary density estimation algorithms have been proposed in recent years [24-27].

This paper addresses the problem of density compensation and presents an improved algorithm based on partial Voronoi diagrams [28, 29]. The proposed method reduces the computational intensity manifold and provides higher fidelity compared to the existing techniques. The algorithm is applied to a simulated image to demonstrate its performance visually, while the corresponding point spread functions are calculated to evaluate the reconstruction quality.

II. The Data Gridding Process

Consider a two-dimensional function $m(x,y)$ whose Fourier

transform is given by

$$M(\omega_x,\omega_y)=\int_{-\infty}^{\infty} m(x,y)e^{-j2\pi(\omega_x x+\omega_y y)}dxdy. \quad (1)$$

If a two-dimensional non-Cartesian sampling function

$$S(\omega_x,\omega_y)=\sum_k {}^2\delta(\omega_x-\omega_{x,k},\omega_y-\omega_{y,k}) \quad (2)$$

samples *m(x, y)*, the result is

$$M_s(\omega_x,\omega_y)=M(\omega_x,\omega_y)S(\omega_x,\omega_y). \quad (3)$$

This is then convolved with the gridding kernel $C(\omega_x, \omega_y)$,

$$M_{sc}(\omega_x,\omega_y)=M_s(\omega_x,\omega_y)*C(\omega_x,\omega_y) \quad (4)$$

where * denotes two-dimensional convolution. It is then sampled on a uniformly-spaced grid to yield

$$\hat{M}(\omega_x,\omega_y)=III(\omega_x,\omega_y)M_{sc}(\omega_x,\omega_y) \quad (5)$$

where $III(\omega_x, \omega_y)$ is the two-dimensional comb function and is defined as a two-dimensional set of equally-spaced delta functions:

$$III(\omega_x,\omega_y)=\sum_a\sum_b {}^2\delta(\omega_x-a,\omega_y-b). \quad (6)$$

The inverse Fourier transform of (5) gives

$$\hat{m}(x,y)=III(x,y)*\left[m_s(x,y)c(x,y)\right] \quad (7)$$

where

$$m_s(x,y)=m(x,y)*s(x,y). \quad (8)$$

Eq. (7) shows the effect of these operations on the reconstructed image in the spatial domain. Any aliasing due to $s(x, y)$ cannot be removed, but non-uniform sampling density can be corrected with an area density correction function $\rho(\omega_x, \omega_y)$ with differential area density according to the sampling density such that it has a higher value at the oversampled regions than the undersampled regions. Two approaches are possible for the calculation of $\rho(\omega_x, \omega_y)$. Pre-compensation calculates the density of each point prior to the gridding operation, mathematically represented by

$$\hat{M}(\omega_x,\omega_y)=III(\omega_x,\omega_y)\left[\frac{M_s(\omega_x,\omega_y)}{\rho(\omega_x,\omega_y)}*C(\omega_x,\omega_y)\right], \quad (9)$$

while in post-compensation, density compensation succeeds gridding, i.e.,

$$\hat{M}(\omega_x,\omega_y)=\frac{1}{\rho(\omega_x,\omega_y)}III(\omega_x,\omega_y)M_{sc}(\omega_x,\omega_y). \quad (10)$$

The latter performs well if the rate of change of the density pattern is not too high. Both techniques can also be applied in conjunction. The image is apodized by the transform of the gridding kernel. Fourier-domain Cartesian sampling causes sidelobe interference in the image space due to the *sinc* sidelobes of the finite gridding kernel. It can be restricted to a region of interest through a two-dimensional *rect(x,y)* function where

$$rect(x,y)=\begin{cases}1 & \text{if } |x|<0.5 \text{ and } |y|<0.5\\ 0 & \text{otherwise}\end{cases}. \quad (11)$$

Deapodization removes the gridding kernel apodization in the image space to obtain $\hat{m}(x,y)$ which is the inverse Fourier transform of equation (9) or (10), i.e.,

$$\bar{m}(x,y)=\hat{m}(x,y)\frac{rect(x,y)}{c(x,y)}. \quad (12)$$

Adjacent replicas can be avoided by sampling the data with sufficient resolution so that the image field-of-view is larger than the actual region of interest [15].

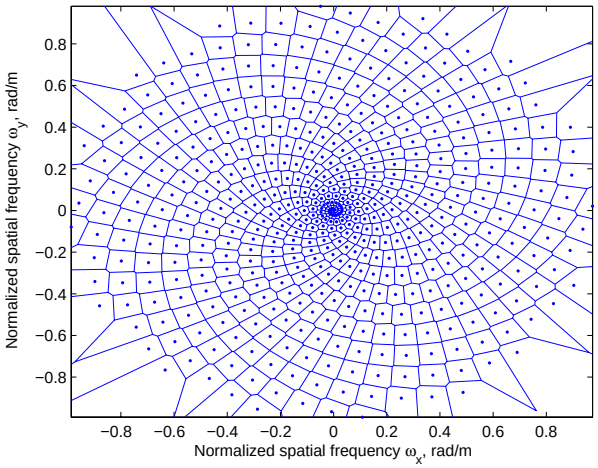

Fig. 1. A Voronoi diagram for a spiral sampling pattern

III. Density Compensation Technique

The algorithm discussed in this paper uses the Voronoi diagram for the estimation of arbitrary sampling density. A similar approach has been reported in [24] for density estimation of samples based on the area they occupy: the Voronoi diagram has been calculated, which gives the cells surrounding every sample point, and the area of each cell is a measure of its density. Fig. 1 shows an example of a Voronoi diagram around spirally distributed data in the Fourier domain. The outer cells tend to be unbounded, and yield incorrectly large, or infinite, areas. To overcome this problem, the convex hull[1] for the sampling points is determined, and points belonging to the outer convex hull are removed. The inner convex hull is determined from the remaining samples and the area of the outer points is assigned by extrapolation using the ratio of the areas of the outer and inner hulls.

Although this is a simple and elegant idea, it adds complexity to the algorithm and is practical only for radial or Cartesian sampling patterns. The QHULL package [30] used for the generation of Voronoi diagram runs with an expected performance of $O(n\log n)$. This appears reasonable in algorithmic terms but is impractical in real-time systems keeping in view the overall processing time of the gridding algorithm of which density estimation is only a small part. Our method improves algorithmic efficiency by limiting the number of points on the dataset for the Voronoi diagram calculation. We calculate the Voronoi area for points close to the centre of the Fourier space, and assign the rest of the points areas equal to that of the last cell in the central Voronoi

[1] The convex hull of a set of points is the smallest convex set containing them

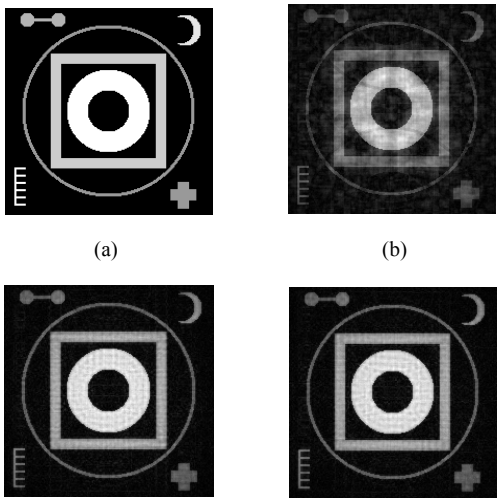

(a) (b) (c) (d)

Fig. 2.(a) Original image. Reconstructed image using (b) no density compensation, (c) full Voronoi compensation, and (d) partial Voronoi compensation

diagram. This choice drastically reduces the number of points processed by the Voronoi function. The points close to the centre of the Fourier space correspond to large-scale patterns. As the density estimate does not require uniform spatial frequencies in most applications, the improvement can be obtained at little cost.

IV. Results

The improved density estimation technique is applied to a simulated intensity image for a visual demonstration of the algorithm's performance. The original image, shown in Fig. 2(a), is constructed such that it contains various intensity levels, sharp edges and sufficient detail. The Fourier transform of the image is then resampled non-uniformly in an arbitrary fashion to create the input data for gridding. It is ensured that this data set has no Nyquist holes since the reconstruction

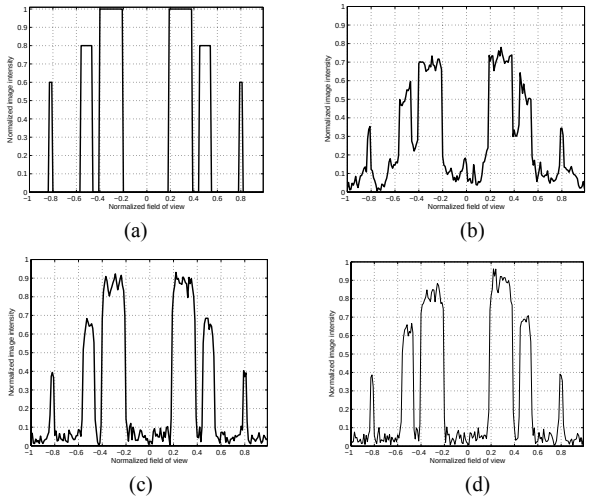

(a) (b) (c) (d)

Fig. 3. Cross-sectional intensity profiles of (a) original image; reconstructed image using (b) no density compensation, (c) full Voronoi compensation, and (d) partial Voronoi compensation

procedure does not perform well with under-sampling [26]. Fig. 2(b) is the result of gridding reconstruction without density correction, while Fig. 2(c) and (d) show the results for full and partial Voronoi reconstruction respectively. The optimal convolution kernel [15] has been used for the reconstruction in the last two cases. The image is randomly distorted in the absence of any density compensation, while the quality of the full and partial resampling images is comparable. Adjusting the kernel width and varying the grid oversampling size to avoid aliasing yields a reconstructed image comparable to the pristine image of Fig. 2(a).

This is further elucidated in Fig. 3 in terms of the cross-sectional intensity profiles taken at the centre of the image. In particular, the profiles in Fig. 3(c) and (d) exhibit strong similarity and are significantly improved compared to Fig. 3(b). Thus high quality reconstruction is achieved, keeping in mind that Fourier sampling for the input image is completely arbitrary. In Fig. 2(d) and 3(d) with partial Voronoi density compensation, only the central $1/4^{th}$ of the points in one

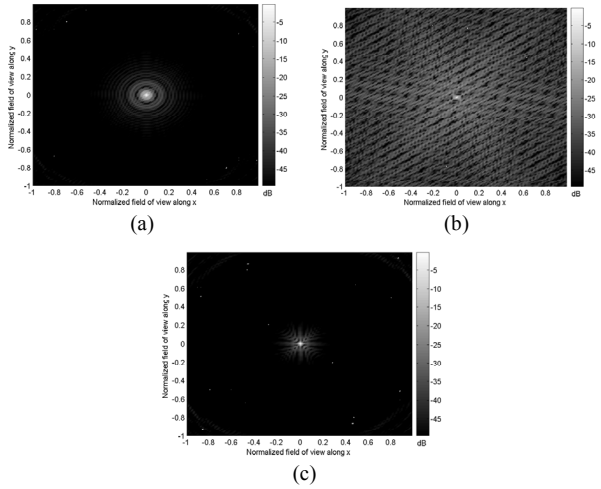

(a) (b) (c)

Fig. 4. Two-dimensional point spread function (impulse response) using: (a) No density compensation, (b) full Voronoi compensation, and (c) partial Voronoi compensation

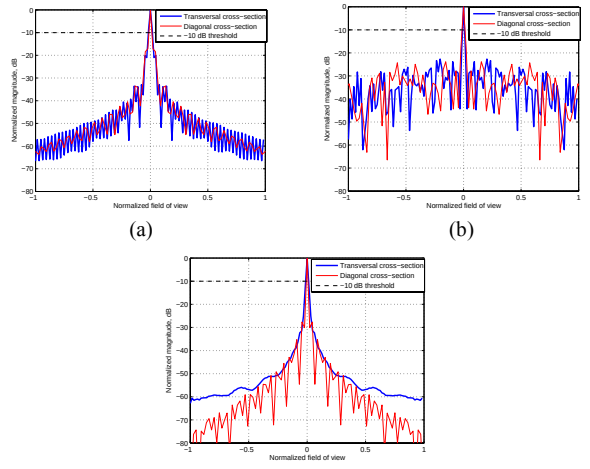

(a) (b) (c)

Fig. 5. Central cross-section of the point spread function using: (a) No density compensation, (b) full Voronoi compensation, and (c) partial Voronoi compensation

TABLE I
10 DB WIDTH OF GRIDDING RECONSTRUCTION POINT SPREAD FUNCTION

Density Estimation Method	Transveral Cross-Section	Diagonal Cross-Section
None	1.75 %	1.29 %
Full Voronoi	0.86 %	1.27 %
Partial Voronoi	1.28 %	0.73 %

TABLE II
PEAK SIDELOBE LEVEL OF GRIDDING RECONSTRUCTION POINT SPREAD FUNCTION

Density Estimation Method	Maximum Sidelobe Level
None	-20 dB
Full Voronoi	-24 dB
Partial Voronoi	-28 dB

direction ($1/16^{th}$ of the Fourier-space data points) have been used to generate the Vornoi diagram, yielding a complexity improvement of 16*log16 = 64 times.

The point spread functions (PSFs) of the gridding reconstruction methods are evaluated to quantify their performance. The two-dimensional PSFs are shown in Fig. 4 in logarithmic scale. In each of the three reconstruction cases, the sidelobe level is well below 10 dB. It is clear that the partial Voronoi PSF, shown in Fig. 4(c), is closest to the ideal PSF. This is further illustrated in Fig. 5 by means of diagonal and transversal cross-sections of the PSFs, which are then used to calculate the corresponding values of the 10 dB width and maximum sidelobe levels. The partial Voronoi technique yields the narrowest PSF, and its sidelobes are 4 dB lower than those of the full Voronoi method. Tables I and II summarize these results and provide evidence of the superior performance of the partial Voronoi resampling technique through lower spreading and higher sidelobe suppression.

V. CONCLUSION

A density estimation method based on the Voronoi diagram is proposed for use in gridding applications where uniform sample data is not available. A partial Voronoi diagram is calculated for Fourier-domain density estimation with an appropriate convolution kernel. This reduced calculation results in a substantially improved computational efficiency than existing methods while also improving the quality of reconstruction.

REFERENCES

[1] L. Chen and D. J. Edwards, "Applications of non-uniform sampling techniques and fast Fourier transform in plane near field antenna measurements," in *Proc. 8th IEE ICAP*. Edinburgh, UK, March 1993.

[2] H. A. Khan, W. Q. Malik, D. J. Edwards, and C. J. Stevens, "Ultra wideband synthetic aperture image formation techniques," in *Proc. IEE UWBCTSD*. London, UK, 8 July 2004.

[3] D. J. Edwards and A. J. Keane, "Numerical techniques for efficient sonar bearing and range searching in the near field using genetic algorithms," in *Evolutionary algorithms in engineering applications*, D. Dasgupta and Z. Michalewicz, Eds. New York, USA: Springer-Verlag, 1997.

[4] H. A. Khan, W. Q. Malik, D. J. Edwards, and C. J. Stevens, "Ultra wideband multiple-input multiple-output radar," in *Proc. IEEE Intl. Radar Conf.* Arlington, VA, USA, 9 May 2005.

[5] J. W. Cooley and J. W. Tukey, "An algorithm for the machine calculation of complex Fourier series," *Mathemat. Comput.*, vol. 19, 1965.

[6] J. Clark, M. Palmer, and P. Lawrence, "A transformation method for the reconstruction of functions from nonuniformly spaced samples," *IEEE Trans. Acoust., Speech, Signal Processing*, vol. ASSP-33, 1985.

[7] H. Stark, J. W. Woods, I. Paul, and R. Hingorani, "Direct Fourier reconstruction in computer tomography," *IEEE Trans. Acoust., Speech, Signal Processing*, vol. ASSP-29, 1981.

[8] S. X. Pan and A. C. Kak, "A computational study of reconstruction algorithms for diffraction tomography: interpolation versus filtered backpropagation," *IEEE Trans. Acoust., Speech, Signal Processing*, vol. ASSP-31, 1983.

[9] J. D. O'Sullivan, "A fast sinc function for Fourier inversion in computer tomography," *IEEE Trans. Med. Imag.*, vol. MI-4, 1985.

[10] H. Sedarat and D. G. Nishimura, "On the optimality of the gridding reconstruction algorithm," *IEEE Trans. Med. Imag.*, vol. 19, April 2000.

[11] N. C. Mathur, "A pseudodynamic programming technique for the design of correlator supersynthesis arrays," *Radio Sci.*, vol. 4, 1969.

[12] D. E. Hogg, G. H. MacDonald, R. G. Conway, and C. M. Wade, "Synthesis of brightness distribution in radio sources," *Astronom. J.*, vol. 74, 1969.

[13] B. Alder, S. Fernbach, and M. Rotenberg, "Aperture synthesis," in *Methods in Computational Physics*, vol. 14. New York, 1975.

[14] H. Moriguchi and J. L. Duerk, "Iterative next-neighbour regridding (INNG): improved reconstruction from nonuniformly sampled k-space data using rescaled matrices," *Magn Reson Med*, vol. 51, February 2004.

[15] J. I. Jackson, C. H. Meyer, D. G. Nishimura, and A. Macovski, "Selection of a convolution function for Fourier inversion using gridding," *IEEE Trans. Med. Imag.*, vol. 10, September 1991.

[16] A. R. Thompson and R. N. Bracewell, "Interpolation and Fourier transformation of fringe visibilities," *Astronom. J.*, vol. 79, 1974.

[17] A. B. Kerr, J. M. Pauly, B. S. Hu, K. C. Li, C. J. Hardy, C. H. Meyer, A. Macovski, and D. G. Nishmura, "Real-time interactive MRI on a conventional scanner," *Magn. Reson. Med.*, vol. 38, 1997.

[18] J. R. Liao, J. M. Pauly, and N. J. Pelc, "MR imaging using piecewise-linear spiral trajectories," in *Proc. 4th Meeting ISMRM*, 1996.

[19] J. R. Liao and N. J. Pelc, "Image reconstruction of generalized spiral trajectories," in *Proc. 4th Meeting ISMRM*, 1996.

[20] C. H. Meyer, B. S. Hu, D. G. Nishimura, and A. Makaovski, "Fast spiral coronary artery imaging," *Magn. Reson. Med.*, vol. 28, 1992.

[21] D. C. Noll, J. A. Webb, and T. E. Warfel, "Parallel data resampling and Fourier inversion by the scane-line method," *IEEE Trans. Med. Imag.*, vol. 14, 1995.

[22] P. Irarrazabal and D. G. Nishimura, "Fast three dimensional magnetic resonance imaging," *Magn. Reson. Med.*, vol. 33, 1995.

[23] R. D. Hoge, R. K. S. Kwan, and G. B. Pike, "Density compensation functions for spiral MRI," *Magn. Reson. Med.*, vol. 38, 1997.

[24] V. Rasche, R. Proksa, R. Sinkus, P. Bornert, and H. Eggers, "Resampling of data between arbitrary grids using convolution interpolation," *IEEE Trans. Med. Imag.*, vol. 18, May 1999.

[25] P. A. Penczek, R. Renka, and H. Schomberg, "Gridding-based direct Fourier inversion of the three-dimensional ray transform," *J. Opt. Soc. Am. A*, vol. 21, April 2004.

[26] J. G. Pipe, "Reconstructing MR images from undersampled data: data-weighting considerations," *Magn. Reson. Med.*, vol. 43, June 2000.

[27] J. G. Pipe and P. Menon, "Sampling density compensation in MRI: rationale and an iterative numerical solution," *Magn. Reson. Med.*, vol. 41, 1999.

[28] M. G. Voronoi, "Nouvelles applications des parameters continus a la theorie des formes quardratiques," *J. Reine Angew. Math.*, vol. 134, 1908.

[29] F. Aurenhammer, "Voronoi Diagrams-A survey of a fundamental data structure," *ACM Compu. Surveys*, vol. 23, pp. 345-405, 1991.

[30] "QHULL," National Science and Technology Research Center for Computation and Visualization of Geometric Structures (The Geometry Center), University of Minnesota, 1993.